

Effect of Doping Nano Samarium(III) Oxide in PVA+Na₃C₆H₅O₇ Films for Battery Applications

J. RAMESH BABU^{1,*}, K. RAVINDHRANATH² and K. VIJAYA KUMAR³

¹Department of Physics, Koneru Lakshmaiah Education Foundation, Vaddeswaram-522502, India

²Department of Chemistry, Koneru Lakshmaiah Education Foundation, Vaddeswaram-522502, India

³Department of Physics, Dayananda Sagar University, Bengaluru-560068, India

*Corresponding author: E-mail: jallirameshura@gmail.com

Received: 13 February 2020;

Accepted: 2 May 2020;

Published online: 27 July 2020;

AJC-19972

The effect of doping nano Sm₂O₃ particles in PVA + Na₃C₆H₅O₇ (90:10% w/w) polymer composite films on the structural, thermal, electrical properties and battery parameters are investigated. The PVA + Na₃C₆H₅O₇ + nano Sm₂O₃ (90:10:1-4% w/w) films were synthesized and characterized. A 2% w/w Sm₂O₃ film was relatively homogeneous with high amorphous in nature enabled the movement of nanoparticles in the matrix of polymer under potential gradient. The maximum conductivity was $2.09 \times 10^{-3} \text{ S cm}^{-1}$ for 2% w/w nano Sm₂O₃ film and it is 7 orders more than polyvinyl alcohol. The films were adopted in batteries with configuration: Anode (Mg+MgSO₄) / [PVA:Na₃C₆H₅O₇ (90:10% w/w) + nano Sm₂O₃ (1-4% w/w)]/cathode (iodine + carbon + pieces of electrolyte) and battery parameters were assessed. The discharge time is 174 h with the cell having 2.0% w/w nano Sm₂O₃ film. These nano Sm₂O₃ doped films are successfully adopted in the fabrication of batteries and also the proposed cells are simple, effective, eco-friendly and economical.

Keywords: Polymer Electrolytes, Polyvinyl alcohol, Nano Sm₂O₃, Battery applications.

INTRODUCTION

Solid polymer electrolytes are important ingredients of batteries, super capacitors, electro-chromic displays, *etc.* They have the hybrid characteristics of ceramic materials and liquid electrolytes with wide applications [1-5]. Investigations to improve conductivity of the solid polymers that are mechanically, thermally and chemically stable are one of the interesting areas of solid state ionics. Modifying the surface of polymer by treating chemically to improve the conductivity of the polymer is an important approach however, it is costly. Hence, composite films embedded with salts and a substance with an endeavor to improve conductivity of the wafers/films is a good approach.

Due to its stable elastic films that withstand temperature and mechanical wearing, polyvinyl alcohol (PVA) is one of the best preference polymer among the researchers. However, they are less conductive, in order to improve its conductivity, investigations are being made by compositing it with more conductive materials. One of the main criteria for choosing such materials is that they are chemically similar or at least possess similar polar groups so that homogeneous films are

resulted [6-8]. Increasing trend in the recent research in this aspect shows that the advantages of nanoparticles of metal oxides are explored for improving the conductivity and stability of films [9,10]. Nano Al₂O₃, TiO₂, SiO₂ and Fe₂O₃ doped in PVA are investigated for their electro-cell applications [11-25]. Nano Pr₂O₃ doped PVA + Na₃C₆H₅O₇ (90:10% w/w) films are successfully adopted for battery applications [10,26].

The advantages of nanoparticles in films may be attributed to the more surface area, paramagnetism, size that helps the particle to penetrate more into the film and quantum confinements. The intimate contact between the nanoparticles and functional groups of films evoke the coordinating tendencies and thereby influences the conductivity. The films possessing more amorphous regions is advantageous as it creates more path ways for the movement of nanoparticles and thereby, an intimate contacts between the particles and the various functional groups present in the composite film, are resulted. The present investigation deals with the effect of doping nano Sm₂O₃ particles in PVA + Na₃C₆H₅O₇ (90:10% w/w) polymer composite films on the structural, thermal, electrical properties and battery parameters.

EXPERIMENTAL

Poly(vinyl alcohol) (m.w. 85,000), sodium citrate and samarium oxide of A.R. grade were used in this work.

Preparation of nano-Sm₂O₃: Samarium(III) oxide was ball milled for 8 h. Sizes of particles were determined by using Scherrer equation on the XRD pattern. From Table-1, it is revealed that the mean particle size of Sm₂O₃ is 36.97 nm. Wearing in ball milling may led to possible contamination with foreign particles [27-30]. But in the present study, foreign materials were not noticed as per FTIR and XRD spectra of nano-Sm₂O₃ and films. Thus, synthesized nano Sm₂O₃ particles were devoid of contamination and employed in the present investigation.

Preparation of composite films: Composite films are prepared using solution cast technique [31]. Varying weight ratios (1-4% w/w) of the nano-sized Sm₂O₃ were mixed with PVA + sodium citrate (90:10% w/w) in triple distilled water. The resulting solution was stirred for 48 h to get a homogenous solution. Thus obtained blends were cast onto polypropylene dishes. The solution was slowly evaporated to obtain thin films. Then the films were peeled out from dishes and dried in vacuum drier for 24 h at room temperature.

Characterization: FTIR Spectra were recorded using Perkin-Elmer FTIR. XRD Bruker D8 instrument with CuK α radiation for angles between 10° to 80° was used to record spectra. SEM images in the present investigations were recorded using FE-SEM, Carl Zeiss, Ultra 55 model. DSC Q20 V24.11 Build 124 was used to record the thermograms. Using HIOKI3532-50 impedance analyzer, measurements for conductivity were made in the frequency range: 50 Hz to 1MHz by varying the temperature: 303 K to 333 K. Keithley Electrometer was used to determine transference numbers by adopting Wagner's polarization [32] and Wanatabe [33] techniques.

Cell fabrication and discharge studies: Cells were fabricated with the configuration: Anode (Mg+MgSO₄)/composite films/cathode (iodine + carbon + pieces of composite electrolyte film). The battery characteristics *viz.* open circuit voltage (OCV), short circuit current (Sc_c), current density, power density, energy density, discharge time and discharge capacity, *etc.* of the cells for a constant load of 100 K Ω were evaluated at room temperature using HIOKI 3532-50 LCR Hitester.

RESULTS AND DISCUSSION

FTIR analysis: The observed FTIR spectra for films are shown in Fig. 1. Some of the key frequencies are presented in Table-2. The main interesting peak is the stretchings of hydroxyl group (-OH). A broad band in 3581 to 3055 cm⁻¹ region with apex at 3312 cm⁻¹ is observed in polyvinyl alcohol. With the addition of 10% of Na₃C₆H₅O₇ in the film, the peak width is decreased: 3531-3114 cm⁻¹ with apex moving to 3291 cm⁻¹ (lower wave number) as has been described in previous study [26]. Addition of Sm₂O₃ (nano) has markedly affected the position and shape of this band. With 1% w/w of Sm₂O₃, this peak width is decreased to 3458 to 3123 cm⁻¹ with apex moved to 3270 cm⁻¹. It is interesting to observe that this band is almost missing in 2% w/w film. Again the broad bands appeared near to this frequency in 3 and 4% w/w films: 3542 to 2103 cm⁻¹ with apex 3280 cm⁻¹ in 3% w/w film; 3510 to 3135 cm⁻¹ with apex 3291 cm⁻¹ in 4% w/w film. These changes in this band may be due to the interactions between the -OH groups of polyvinyl alcohol, various functional groups of Na₃C₆H₅O₇ and Sm₂O₃. In polyvinyl alcohol, the -OH groups are bounded to each other by hydrogen bridges and they may be either inter or intra-molecular bindings. When Na₃C₆H₅O₇ and Sm₂O₃ are present in film, the bonding between the -OH groups is disturbed due to formation of more and more hydrogen bridges between the polymer, salt and nanoparticles. The bond is vanished completely in 2% film. This indicates the role of Sm=O in the formation of hydrogen bridges of type -O....H....O=Sm. With further increase in the content of Sm₂O₃, the latter are getting accumulated in the matrix because; the film is already saturated at 2% w/w with respect to Sm₂O₃. The appearance of broaden peaks at 3 and 4% w/w may be due to the stretching frequencies of -OH in HO-S=O.

The bands for other functional groups have lower wave-number with the increase in the content of Sm₂O₃ (Fig. 1). These observations of missing and/or shifting of different frequencies of functional groups confirm a sort of complexation between polyvinyl alcohol, Na₃C₆H₅O₇ and nano Sm₂O₃. It seems to be optimum at 2% w/w of nano Sm₂O₃ for producing good and homogeneous film. Defamation bands of HO-Sm=O are observed at 640 cm⁻¹ (1% w/w), 629 cm⁻¹ (2% w/w), 661

TABLE-1
DETERMINATION OF Sm₂O₃ PARTICLE SIZE USING SCHERRER EQUATION

2 θ	θ	cos θ	FWHM (°)	FWHM radian	β cos θ	Size of particle (nm)
23.34	11.67	0.979	0.233	0.00406	0.00398	34.8311228
24.02	12.01	0.978	0.196	0.00342	0.00334	41.4487236
25.9	12.95	0.974	0.187	0.00326	0.00318	43.621995
30.77	15.385	0.964	0.207	0.00361	0.00348	39.816099
35.77	17.885	0.951	0.245	0.00427	0.00406	34.100401
36.19	18.095	0.999	0.24	0.00419	0.00418	33.1382338
37.43	18.715	0.947	0.215	0.00375	0.00355	39.0227299
40.57	20.285	0.937	0.239	0.00417	0.00391	35.4787733
16.45	8.225	0.989	0.195	0.0034	0.00336	41.19791
53.27	26.635	0.893	0.544	0.00949	0.00847	16.3551951
45.32	22.66	0.922	0.242	0.00422	0.00389	35.6090019
42.06	21.03	0.935	0.173	0.00302	0.00282	49.1188707
Average size						36.9782547

TABLE-2
IR DATA: NANO Sm₂O₃ DOPED PVA + Na₃C₆H₅O₇ (90:10% w/w) FILMS

Functional group	Films						
	PVA	PVA + Na ₃ C ₆ H ₅ O ₇ (90:10% w/w)	Nano Sm ₂ O ₃ (% w/w)				Na ₃ C ₆ H ₅ O ₇
			1.0%	2.0%	3.0%	4.0%	
-OH (s)	3581-3055 with apex 3312	3531-3114 with apex 3291	3458 to 3123	Missed	3542 to 2103 cm ⁻¹ with apex 3280 cm ⁻¹	3510 to 3135 with apex 3291	3650, 3436, 3241
-CH ₂ (s)	2944	2921	2909	Missed	2884	2915	2880, 2945
-C-O (s)	1098	1087	1073	Missed	1069	1063	-
Carboxilate ion	-	1715	1705	1694	Missed	1684	-
Sm=O	-	-	640	629	661	639	-

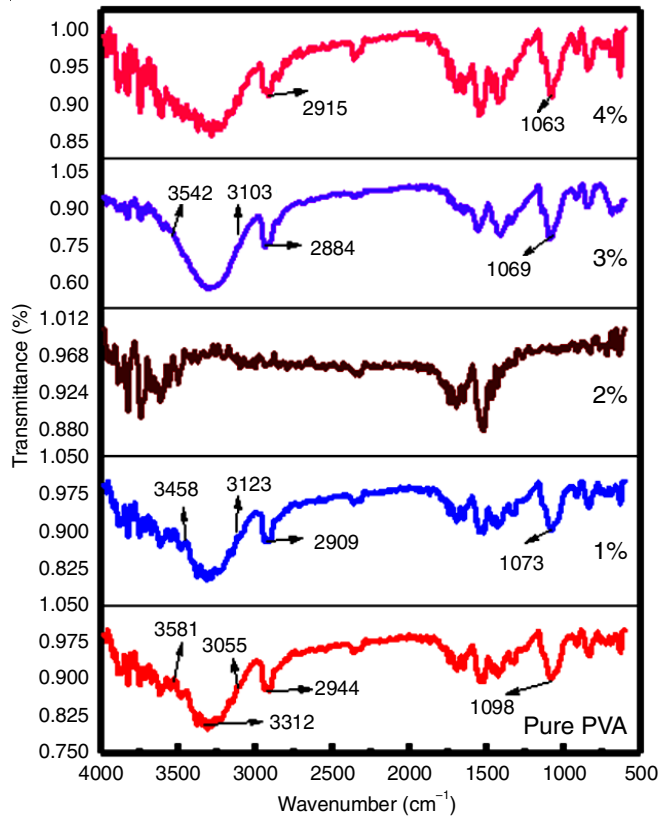


Fig. 1. FTIR spectra of different films: [(PVA + Na₃C₆H₅O₇ (90:10% w/w)) + nano Sm₂O₃ (1-4% w/w)] films

cm⁻¹ (3% w/w), 639 cm⁻¹ (4% w/w) with varying intensities (Table-2). With 2% film, the band intensity is minimum indicating its involvement in the interactions with the other ingredients of the film.

XRD studies: Sharp bands of Sm₂O₃ indicate perfect crystallinity (Fig. 2). PVA shows broad peak: 18-22°, in the 2θ range (110) and this indicates more amorphous region. Adding 10% w/w Na₃C₆H₅O₇ in the film, widen the peaks with the apex moving to 19.0°. This suggests a decrease in crystallinity of the composite film.

When nano-Sm₂O₃ particles are incorporated in the film in different concentrations, the peak is further widened with the shift of maxima towards higher values. With 1% w/w in the film, the apex is moved to 19.17°; with 2%: 19.06°. But with 3 and 4% w/w Sm₂O₃ films though the shift and broadness are observed, sharp bands pertaining to the nano Sm₂O₃ are appearing. This is due to the agglomeration of undissolved

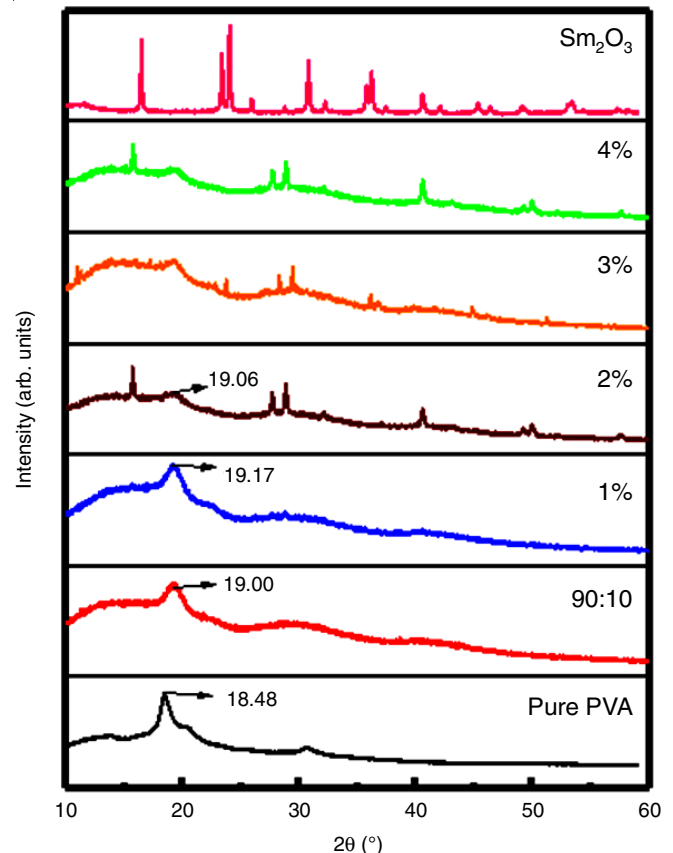


Fig. 2. XRD spectra: neat PVA; PVA:Na₃C₆H₅O₇; (90:10% w/w) + nano Sm₂O₃ (1-4% w/w) films

Sm₂O₃ in the film. Hence, the presence of 2% w/w nano Sm₂O₃ is optimum to have the homogeneous films. At this proportion, all ingredients in this film are thoroughly mixed. This 2% film has more amorphous region than rest of the films. The amorphous regions in the film create more path ways for the movement of nanoparticles and so, intimate contacts between the particles and the various functions groups present in the composite film are resulted. This endows the conducive conditions for enhancement of conductivity.

SEM Studies: Nano Sm₂O₃ dispersal in films can be elucidated from SEM images. The surface morphologies of the films having different nano Sm₂O₃ concentrations were studied using SEM images (Fig. 3). It may be noted that of the all films, 2% w/w film is more homogeneous than the rest. Most of the corners, edges, holes and boundaries have disappeared in 2% w/w film. In other words, crystallinity is less observed in the film at the

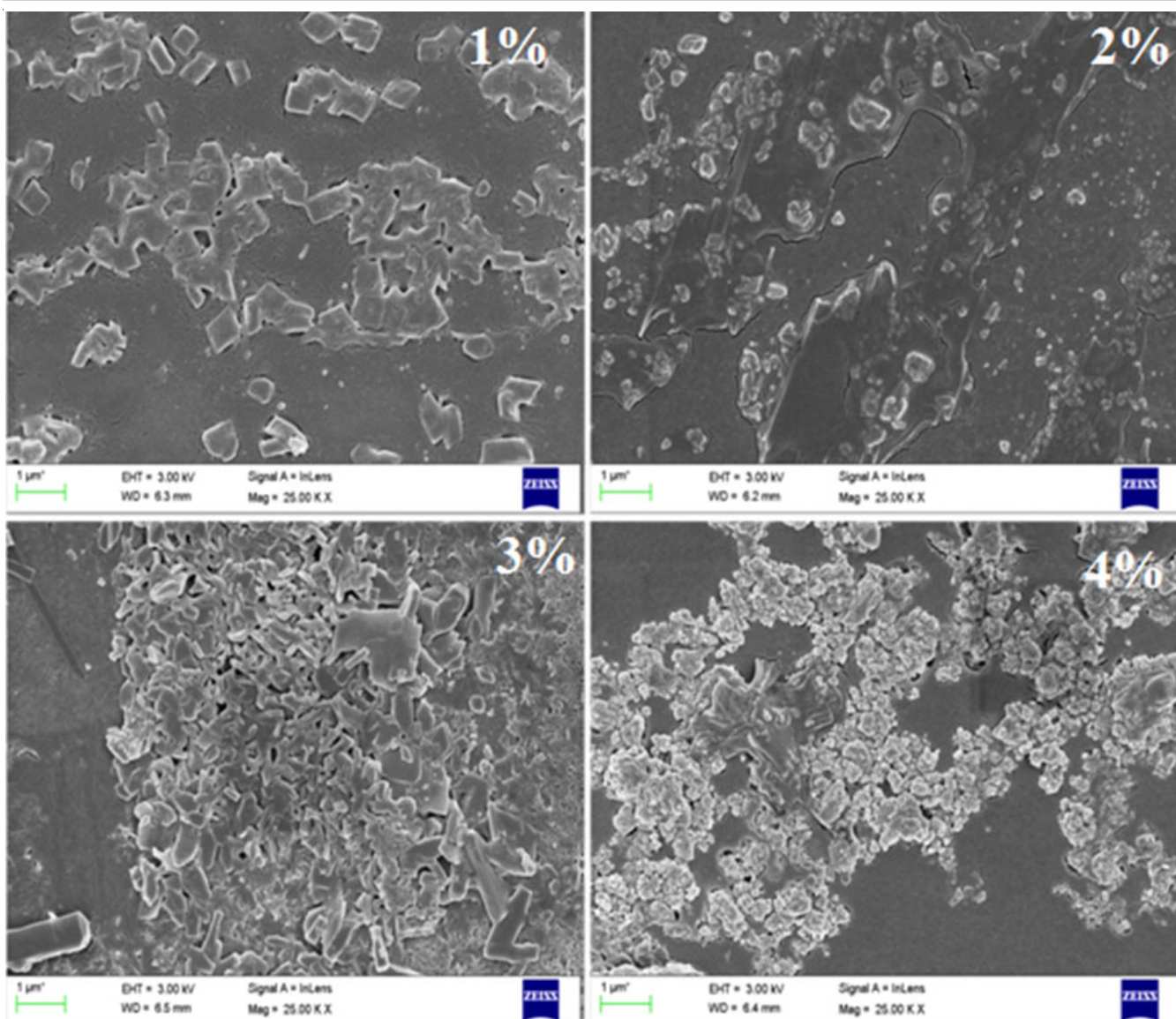


Fig. 3. SEM images of composite films of PVA (90%) + $\text{Na}_3\text{C}_6\text{H}_5\text{O}_7$ (10%) + nano Sm_2O_3 (1-4%)

said proportions. In 3% w/w film, aggregates of crystallinities are observed. Many more crystallites are observed in 4% w/w film. Hence, it may be concluded that at 2% w/w film is saturated with respect to Sm_2O_3 .

As the ingredients of the film namely PVA, $\text{Na}_3\text{C}_6\text{H}_5\text{O}_7$ and nano Sm_2O_3 have structurally similar or nearly similar functional groups ($-\text{OH}$, $\text{C}=\text{O}$, $>\text{O}$, *etc.*), the interactions between them is strong. Further, the Lewis acidic nature of the central metal ion of Sm_2O_3 may also contribute in these interactions by evoking coordinating capacities of the functional groups to occupy the vacant coordination sites of Sm_2O_3 . So, homogeneity in the film is resulted due to these interactions. The homogeneousness of film is maximum in the saturated 2% w/w film. Beyond this percentage, Sm_2O_3 is agglomerating and more crystallites are noticed in 3 and 4% w/w films.

DSC analysis: Thermograms (Fig. 4) of DSC were recorded for all the films of compositions: PVA: $\text{Na}_3\text{C}_6\text{H}_5\text{O}_7$ (90:10% w/w) + Sm_2O_3 (1-4% w/w). It may be inferred that as Sm_2O_3 percen-

tage in the film is increasing upto 2% w/w in films, the m.p., T_g and crystallinity (%) were decreased. But with 3 and 4% w/w films, the values increased. In other words, for 2% w/w film, the values were minimum for all the said parameters: T_g : 90.15 °C; m.p.: 221.85 °C and crystallinity: 72.5% (Table-3). Hence, 2.0% w/w film is relatively more homogeneous and amorphous than the rest of the films. Sm_2O_3 nanoparticles penetrate into the voids among the chains (crystalline) of PVA and bind them *via* functional groups evoking various physico-chemical interactions. When nano Sm_2O_3 concentration increased progressively, the interactions also increased, which lead to the increase in the solubility of all the ingredients of the film and hence, decreasing the tendency of melting point, T_g and crystallinity values. However, when the concentration is more than 2%, the values for the said parameters increased again. This is due to the fact that 2% w/w film is saturated with respect to Sm_2O_3 . More than this percentage, excess Sm_2O_3 was agglomerated and thereby increased the parameters values. Hence,

TABLE-3
DSC STUDIES USING PVA:Na₃C₆H₅O₇:
NANO Sm₂O₃ (1-4%) FILMS

Compositions*	T _g	m.p.	Crystallinity (%)
90:10:1%*	91.38	223.44	74.28
90:10:2%*	90.15	221.85	72.50
90:10:3%*	95.32	225.27	75.34
90:10:4%*	98.14	226.05	76.62
Polyvinyl alcohol	92.98	224.05	100.00

*Polyvinyl alcohol:Na₃C₆H₅O₇:nano Sm₂O₃; % of crystallinities were calculated using the equation [34]. $\% \chi_c = \frac{\Delta H_m}{\Delta H_m^0} \times 100$, where ΔH_m^0 is the melting enthalpy of pure PVA and ΔH_m is melting enthalpy of related Sodium Citrate complexed and/or nano Sm₂O₃ doped PVA films.

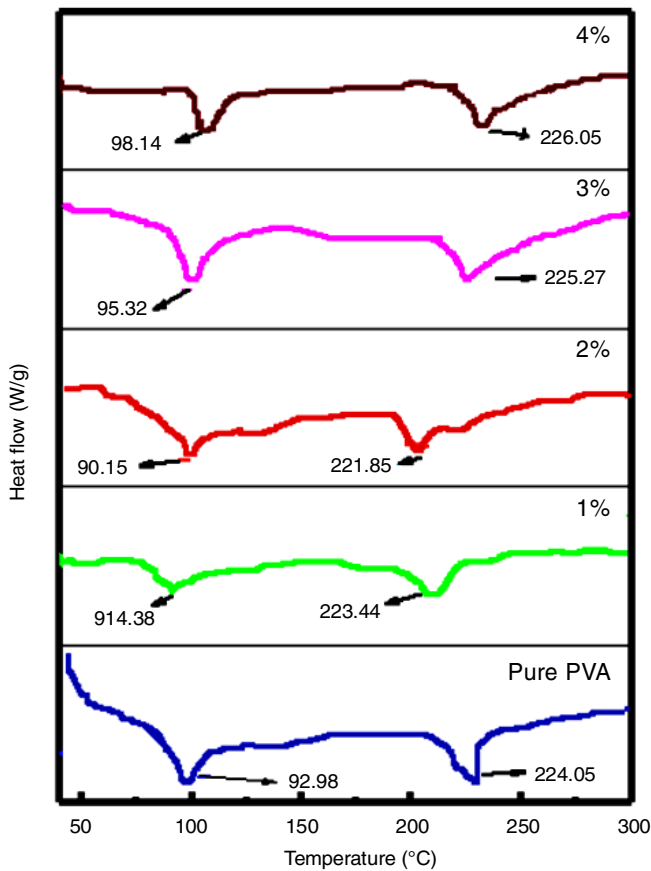


Fig. 4. DSC thermograms of films: PVA; [(PVA:Na₃C₆H₅O₇ (90:10% w/w) + nano Sm₂O₃ (1-4% w/w))]

2% film is found to be more viable for ionic mobility due to its more amorphous nature.

AC conductivity measurements: For all the films, complex impedance (CI) curves were plotted at room temperature (303 K) using HIOKI3532-50 impedance analyzer. Further, complex impedance (CI) curves were noted at different temperatures viz. 303, 308, 313 and 318 K for the film containing optimum 2% nano-Sm₂O₃. The conductivities and activation energies were calculated. The results are presented in Fig. 5a-b and Table-4.

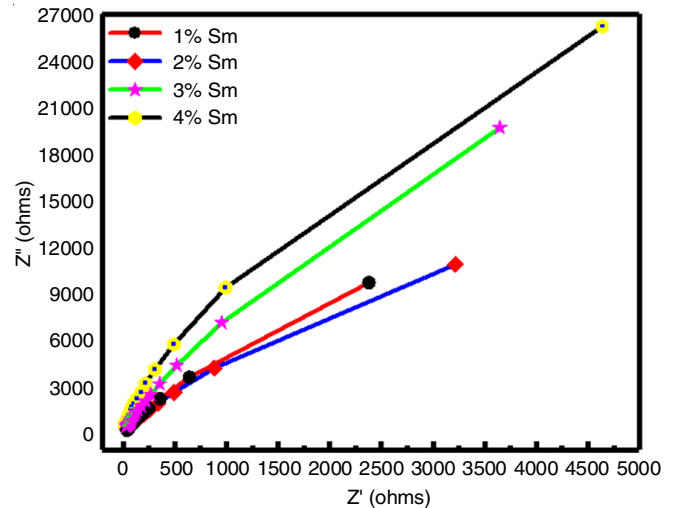


Fig. 5a. Plots of impedance: PVA + Na₃C₆H₅O₇ (90:10%w/w) + nano Sm₂O₃ (1 to 4% w/w) films

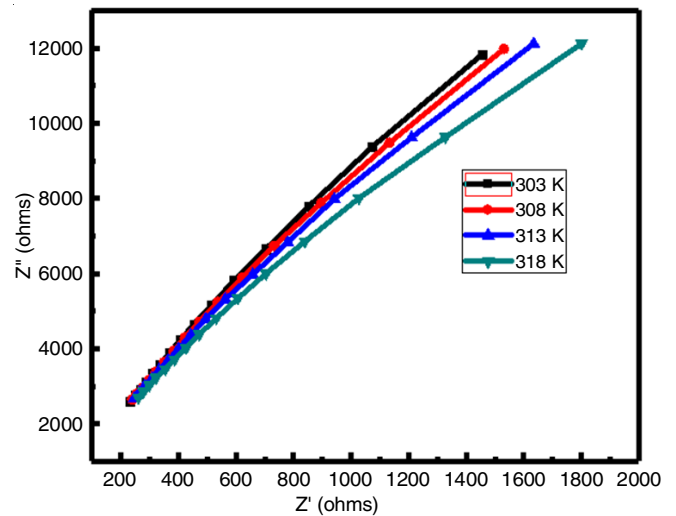


Fig. 5b. Variation of conductivity with temperatures for the film: PVA + Na₃C₆H₅O₇ (90:10% w/w) + 2.0% nano Sm₂O₃

Pure polyvinyl alcohol exhibits a poor conductivity (10⁻¹⁰ S/cm) [35]. However, presence of nano-Sm₂O₃ content in the

TABLE-4
ELECTRICAL PROPERTIES OF THE PVA:Na₃C₆H₅O₇ (90:10 % w/w) + NANO Sm₂O₃ (1-4% w/w) FILMS

Film compositions	A.C. conductivity (S cm ⁻¹) at room temp.: 303 K	E _a	Transport numbers	
			t _{ion}	t _{ele}
Polyvinyl alcohol + Na ₃ C ₆ H ₅ O ₇ (90:10 % w/w) + nano Sm ₂ O ₃ (1.0 % w/w)	8.21 × 10 ⁻⁴	0.30	0.97	0.03
Polyvinyl alcohol + Na ₃ C ₆ H ₅ O ₇ (90:10 % w/w) + nano Sm ₂ O ₃ (2.0 % w/w)	2.09 × 10 ⁻⁴	0.22	0.99	0.01
Polyvinyl alcohol + Na ₃ C ₆ H ₅ O ₇ (90:10 % w/w) + nano Sm ₂ O ₃ (3.0 % w/w)	2.16 × 10 ⁻⁵	0.34	0.98	0.02
Polyvinyl alcohol + Na ₃ C ₆ H ₅ O ₇ (90:10 % w/w) + nano Sm ₂ O ₃ (4.0 % w/w)	5.43 × 10 ⁻⁶	0.36	0.97	0.03
Polyvinyl alcohol	5.59 × 10 ⁻¹⁰	0.42	–	–

films upto 2% w/w in the films has remarkably increased the conductivity to $2.09 \times 10^{-3} \text{ S cm}^{-1}$, which is nearly seven times more than polyvinyl alcohol film. The conductivity is due to the movement of electrons or ions or both. The ionic movement is facilitated in the more amorphous regions of the film. Sm_2O_3 in films alter the micro-structures in the film so as to create more pathways. These additional short pathways enhance conductivity. It may be attributed to the more surface area, size that helps the particle to penetrate more into the film and quantum confinements of nano Sm_2O_3 as discussed earlier in this work. As 2% w/w film has more amorphousness, the film at the said composition exhibits maximum conductivity.

In 3 and 4% w/w film, Sm_2O_3 appears to reduce pathways due to agglomeration (initial stages of precipitation) of the particles and thereby, restricting the ionic movement. Further, agglomerated Sm_2O_3 may also enhance the film's microscopic viscosity, resulting the decrease in conductivity.

It can be inferred from Table-5, with increase in temperature, conductivity of 2% film also increases. Inter-chain and/or intra-chain hopping in the microstructures of the film and also fall in viscosity of the film, favour the movement of ions.

TABLE-5
CONDUCTIVITIES AT DIFFERENT TEMPERATURES:
POLYVINYL ALCOHOL + $\text{Na}_3\text{C}_6\text{H}_5\text{O}_7$ + NANO Sm_2O_3
(90:10:2% w/w) FILM

Temperature (K)	Conductivity (S cm^{-1})
303	2.09×10^{-3}
313	2.84×10^{-3}
323	3.90×10^{-3}
333	5.10×10^{-3}

Transport number measurements: The transport numbers were evaluated using the cell: anode (Ag)/[PVA: $\text{Na}_3\text{C}_6\text{H}_5\text{O}_7$ (90:10% w/w) + 1-4% w/w Sm_2O_3]/cathode (Ag). The findings are shown in Fig. 6. From the data (Table-4), it can be inferred that for all the films, ions are the major carriers of charge. In 2% w/w film having low crystallinity, the activation energy is less and t_{ion} is high. The t_{ion} values for 2% film is nearly to 'unity', which is a good feature for its adoptability in batteries [36-38].

Discharge characteristics: The adoptability of nano Sm_2O_3 doped films in batteries was assessed by fabricating a battery of the composition: anode (Mg+ MgSO_4)/composite films/cathode (iodine + carbon + pieces of composite elect-

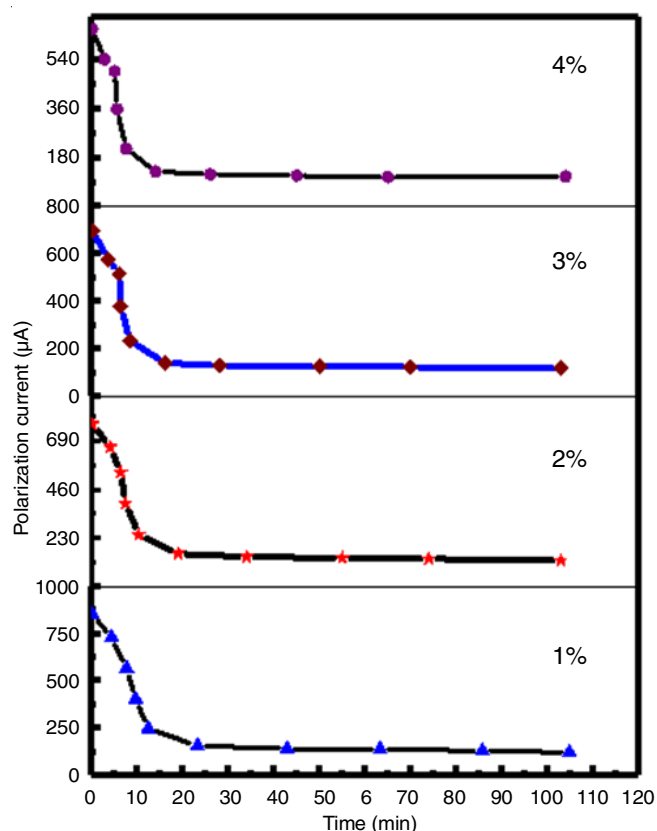


Fig. 6. Transport number measurements for the films containing various amounts (1 to 4% w/w) of Sm_2O_3 in PVA + $\text{Na}_3\text{C}_6\text{H}_5\text{O}_7$ (90:10% w/w) films

rolyte film). Various cell parameters were investigated and the results are shown in Table-6 and Fig. 7.

It is inferred from the data that the cell formed with film containing 2% w/w nano-sized Sm_2O_3 exhibits improved battery characteristics than the rest of the films. The discharge time, power density and energy density of the cell using the film containing 2% w/w of Sm_2O_3 are found to be 174 h, 0.64 w/kg and 111.7 wh/kg, respectively. These features signify the successful adoptability of present nano Sm_2O_3 doped films in batteries.

Comparative studies: The developed battery system is compared with respect to open circuit voltage (OCV) and discharge time with reported similar works. It is revealed from Table-7 that the present developed battery profile is more effective than many hitherto developed battery systems in the

TABLE-6
CELL PARAMETERS USING PVA + $\text{Na}_3\text{C}_6\text{H}_5\text{O}_7$ (90:10 % w/w) + 1-4% NANO Sm_2O_3 % w/w
FILMS [CELL AREA: 1.34 cm^2 ; CELL WEIGHT: 1.40 g]

Cell parameters	1.0 % w/w Sm_2O_3 film*	2.0 % w/w Sm_2O_3 film*	3.0 % w/w Sm_2O_3 film*	4.0 % w/w Sm_2O_3 film*
OCV (Volts)	1.98	1.87	1.78	1.72
Sec (μA)	581	462	540	300
Discharge time (h)	145	174	149	126
Power density (w/kg)	0.82	0.64	0.68	0.36
Energy density (wh/kg)	118.9	111.7	102.21	46.43
Current density ($\mu\text{A}/\text{cm}^2$)	432	344	402	223.8
Discharge capacity (mA-h)	84.1	80.21	80.46	37.8

*PVA + $\text{Na}_3\text{C}_6\text{H}_5\text{O}_7$ (90:10 % w/w) + 1-4% nano Sm_2O_3 % w/w

TABLE-7
COMPARISON OF PRESENT CELLS WITH PREVIOUS INVESTIGATIONS

Configuration	OCV (V)	Discharge time (h)	Ref.
Ag/(PVP + AgNO ₃)/(Iodine + Carbon + pieces of electrolyte)	0.46	82	[32]
Ag/(PEO + AgNO ₃)/(Iodine + Carbon + pieces of electrolyte)	0.61	48	[39]
Na/(PEO + glass)/(Iodine + Carbon + pieces of electrolyte)	2.45	98	[40]
Mg/(PEO + Mg(NO ₃) ₂)/(Iodine + Carbon + pieces of electrolyte)	1.85	142	[41]
Na/(PVA + NaF)/(Iodine + Carbon + pieces of electrolyte)	2.53	122	[42]
K/(PVP + PVA + KBrO ₃)/(Iodine + Carbon + pieces of electrolyte)	2.30	72	[43]
Mg/PVA + Mg(CH ₃ COO) ₂ /(Iodine + Carbon + pieces of electrolyte)	1.84	87	[44]
Mg + MgSO ₄ /[{PVA + Na ₃ C ₆ H ₅ O ₇ (90:10% w/w)} + nanoSm ₂ O ₃ 2.0 % w/w]/(Iodine + Carbon + pieces of electrolyte)	1.87	174	Present study

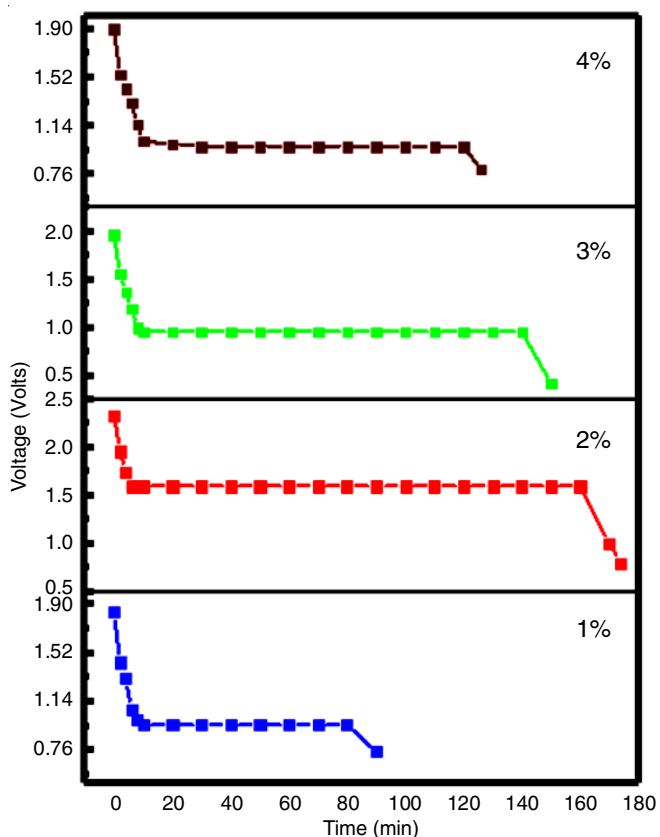


Fig. 7. Discharge characteristic plots of batteries having 'PVA + Na₃C₆H₅O₇ (90:10% w/w)' films doped with Sm₂O₃ (1-4%w/w)

aspects of discharge time and open circuit voltage. These features emphasize the successful adoptability of the present developed nano based films in the electrochemical cells. Furthermore, the proposed cell is simple, effective, eco-friendly and economical.

Conclusion

Polymeric composite films were synthesized by incorporating different concentrations (1 to 4% w/w) nano-Sm₂O₃ in PVA + Na₃C₆H₅O₇ (90:10% w/w). Structural, thermal and electrical properties are assessed by various techniques. A 2% w/w Sm₂O₃ film was relatively more homogeneous and exhibited a high amorphousness. This enables to have intimate contact and facilitate more interactions with the various functional groups in the composite. This is an ideal environment for the movement of nanoparticles in the matrix of polymer under potential gradient. A maximum conductivity of 2.09×10^{-3} S

cm⁻¹ exhibited by 2% nano Sm₂O₃ film, which is nearly seven times more than polyvinyl alcohol film. The developed films were also adopted in batteries with configuration: Anode (Mg+MgSO₄)/[{PVA: Na₃C₆H₅O₇ (90:10% w/w)} + nano Sm₂O₃ (1-4% w/w)]/Cathode (iodine + carbon + pieces of electrolyte) and investigated for various battery characteristics. The maximum discharge time was found to be 174 h with the battery having 2% w/w nano Sm₂O₃ film. The nano Sm₂O₃ films developed in the present work is successfully adopted in the fabrication batteries.

CONFLICT OF INTEREST

The authors declare that there is no conflict of interests regarding the publication of this article.

REFERENCES

- J.C. Lasseques and P. Colombon, Proton Conductors: Solids, Membranes and Gels, University Press: Cambridge (1992).
- C.S. Ramya, S. Selvasekarapandian, T. Savitha, G. Hirankumar, R. Baskaran, M.S. Bhuvanewari and P.C. Angelo, *Eur. Polym. J.*, **42**, 2672 (2006); <https://doi.org/10.1016/j.eurpolymj.2006.05.020>
- B. Smitha, S. Sridhar and A.A. Khan, *J. Membr. Sci.*, **259**, 10 (2005); <https://doi.org/10.1016/j.memsci.2005.01.035>
- N. Srivastava and S. Chandra, *Eur. Polym. J.*, **36**, 421 (2000); [https://doi.org/10.1016/S0014-3057\(99\)00056-7](https://doi.org/10.1016/S0014-3057(99)00056-7)
- H.T. Pu and D. Wang, *Electrochim. Acta*, **51**, 5612 (2006); <https://doi.org/10.1016/j.electacta.2006.02.035>
- M.M. Coleman and P.C. Painter, *Prog. Polym. Sci.*, **20**, 1 (1995); [https://doi.org/10.1016/0079-6700\(94\)00038-4](https://doi.org/10.1016/0079-6700(94)00038-4)
- T. Kanbara, M. Inami and T. Yamamoto, *J. Power Sources*, **36**, 87 (1991); [https://doi.org/10.1016/0378-7753\(91\)80047-2](https://doi.org/10.1016/0378-7753(91)80047-2)
- H.A. Every, F. Zhou, M. Forsyth and D.R. MacFarlane, *Electrochim. Acta*, **43**, 1465 (1998); [https://doi.org/10.1016/S0013-4686\(97\)10085-8](https://doi.org/10.1016/S0013-4686(97)10085-8)
- D. Kumar and S.A. Hashmi, *J. Power Sources*, **195**, 5101 (2010); <https://doi.org/10.1016/j.jpowsour.2010.02.026>
- J. Ramesh Babu, K. Ravindhranath and K. Vijaya Kumar, *Int. J. Polym. Sci.*, **2018**, 7906208 (2018); <https://doi.org/10.1155/2018/7906208>
- F. Croce, L. Persi, B. Scrosati, F. Serraino-Fiory, E. Plichta and M.A. Hendrickson, *Electrochim. Acta*, **46**, 2457 (2001); [https://doi.org/10.1016/S0013-4686\(01\)00458-3](https://doi.org/10.1016/S0013-4686(01)00458-3)
- Z. Li, G. Su, D. Gao, X. Wang and X. Li, *Electrochim. Acta*, **49**, 4633 (2004); <https://doi.org/10.1016/j.electacta.2004.05.018>
- C.C. Tambelli, A.C. Bloise, A.V. Rosário, E.C. Pereira, C.J. Magon and J.P. Donoso, *Electrochim. Acta*, **47**, 1677 (2002); [https://doi.org/10.1016/S0013-4686\(01\)00900-8](https://doi.org/10.1016/S0013-4686(01)00900-8)
- P.A.R.D. Jayatilaka, M.A.K.L. Dissanayake, I. Albinsson and B.-E. Mellander, *Electrochim. Acta*, **47**, 3257 (2002); [https://doi.org/10.1016/S0013-4686\(02\)00243-8](https://doi.org/10.1016/S0013-4686(02)00243-8)

15. M.A.K.L. Dissanayake, P.A.R.D. Jayathilaka, R.S.P. Bokalawala, I. Albinsson and B.-E. Mellander, *J. Power Sources*, **119–121**, 409 (2003); [https://doi.org/10.1016/S0378-7753\(03\)00262-3](https://doi.org/10.1016/S0378-7753(03)00262-3)
16. C.H. Park, D.W. Kim, J. Prakash and Y.-K. Sun, *Solid State Ion.*, **159**, 111 (2003); [https://doi.org/10.1016/S0167-2738\(03\)00025-0](https://doi.org/10.1016/S0167-2738(03)00025-0)
17. B. Kumar, S.J. Rodrigues and S. Koka, *Electrochim. Acta*, **47**, 4125 (2002); [https://doi.org/10.1016/S0013-4686\(02\)00442-5](https://doi.org/10.1016/S0013-4686(02)00442-5)
18. Y. Liu, J.Y. Lee and L. Hong, *J. Power Sources*, **109**, 507 (2002); [https://doi.org/10.1016/S0378-7753\(02\)00167-2](https://doi.org/10.1016/S0378-7753(02)00167-2)
19. L. Fan, *Solid State Ion.*, **164**, 81 (2003); <https://doi.org/10.1016/j.ssi.2003.08.004>
20. H.M. Xiong, K.K. Zhao, X. Zhao, Y.W. Wang and J.S. Chen, *Solid State Ion.*, **159**, 89 (2003); [https://doi.org/10.1016/S0167-2738\(02\)00917-7](https://doi.org/10.1016/S0167-2738(02)00917-7)
21. L. Fan, Z. Dang, G. Wei, C.-W. Nan and M. Li, *Mater. Sci. Eng. B*, **99**, 340 (2003); [https://doi.org/10.1016/S0921-5107\(02\)00487-7](https://doi.org/10.1016/S0921-5107(02)00487-7)
22. J. Adebahr, N. Byrne, M. Forsyth, D.R. MacFarlane and P. Jacobsson, *Electrochim. Acta*, **48**, 2099 (2003); [https://doi.org/10.1016/S0013-4686\(03\)00191-9](https://doi.org/10.1016/S0013-4686(03)00191-9)
23. B. Kumar, S.J. Rodrigues and L.G. Scanlon, *J. Electrochem. Soc.*, **148**, A1191 (2001); <https://doi.org/10.1149/1.1403729>
24. J.D. Kim and I. Honma, *Electrochim. Acta*, **48**, 3633 (2003); [https://doi.org/10.1016/S0013-4686\(03\)00484-5](https://doi.org/10.1016/S0013-4686(03)00484-5)
25. A. D'Epifanio, F.S. Fiory, S. Licocchia, E. Traversa, B. Scrosati and F. Croce, *J. Appl. Electrochem.*, **34**, 403 (2004); <https://doi.org/10.1023/B:JACH.0000016623.42147.68>
26. J.R. Babu, K. Ravindhranath and K.V. Kumar, *Asian J. Chem.*, **29**, 1049 (2017); <https://doi.org/10.14233/ajchem.2017.20405>
27. M. Ristic, I. Nowik, S. Popovic, I. Felner and S. Music, *Mater. Lett.*, **57**, 2584 (2003); [https://doi.org/10.1016/S0167-577X\(02\)01315-0](https://doi.org/10.1016/S0167-577X(02)01315-0)
28. G. Stefanic, S. Music and A. Gajovic, *Mater. Res. Bull.*, **41**, 764 (2006); <https://doi.org/10.1016/j.materresbull.2005.10.006>
29. G. Stefanic, S. Music and A. Gajovic, *J. Eur. Ceram. Soc.*, **27**, 1001 (2007); <https://doi.org/10.1016/j.jeurceramsoc.2006.04.136>
30. S.G. Sarwat, *Powder Metall.*, **60**, 267 (2017); <https://doi.org/10.1080/00325899.2017.1280647>
31. M. White, *Thin Solid Films*, **18**, 157 (1973); [https://doi.org/10.1016/0040-6090\(73\)90095-3](https://doi.org/10.1016/0040-6090(73)90095-3)
32. J.B. Wagner and C.J. Wagner, *J. Chem. Phys.*, **26**, 1597 (1957); <https://doi.org/10.1063/1.1743590>
33. M. Watanabe, S. Nagano, K. Sanui and N. Ogata, *Solid State Ion.*, **28**, 911 (1988); [https://doi.org/10.1016/0167-2738\(88\)90303-7](https://doi.org/10.1016/0167-2738(88)90303-7)
34. M. Hema, S. Selvasekerapandian, G. Hirankumar, A. Sakunthala, D. Arunkumar and H.J. Nithya, *Phys. Chem. Solids*, **70**, 1098 (2009); <https://doi.org/10.1016/j.jpics.2009.06.005>
35. A. Lewandowski, M. Zajder, E. Frackowiak and F. Beguin, *Electrochim. Acta*, **46**, 2777 (2001); [https://doi.org/10.1016/S0013-4686\(01\)00496-0](https://doi.org/10.1016/S0013-4686(01)00496-0)
36. P.S. Anantha and K. Hariharan, *Solid State Ion.*, **176**, 155 (2005); <https://doi.org/10.1016/j.ssi.2004.07.006>
37. M. Watanabe, S. Nagano, K. Sanui and N. Ogata, *Solid State Ion.*, **18–19**, 338 (1986); [https://doi.org/10.1016/0167-2738\(86\)90137-2](https://doi.org/10.1016/0167-2738(86)90137-2)
38. B.B. Owens, *Adv. Electrochem. Electrochem. Eng.*, **8**, 1 (1971).
39. S. Sreepathirao, K. Satyanarayanan, M. Shareefuddin, U. Subbarao and S. Chandra, *Solid State Ion.*, **67**, 331 (1994); [https://doi.org/10.1016/0167-2738\(94\)90026-4](https://doi.org/10.1016/0167-2738(94)90026-4)
40. M. Jaipal Reddy and U.V.S. Rao, *J. Mater. Sci. Lett.*, **17**, 1613 (1998); <https://doi.org/10.1023/A:1006600802298>
41. M.A. Ratner and D.F. Shriver, *Chem. Rev.*, **88**, 109 (1988); <https://doi.org/10.1021/cr00083a006>
42. P.B. Bhargav, V.M. Mohan, A.K. Sharma and V.V.R.N. Rao, *Curr. Appl. Phys.*, **9**, 165 (2009); <https://doi.org/10.1016/j.cap.2008.01.006>
43. R.M. Hodge, G.H. Edward and G.P. Simon, *Polymer*, **37**, 1371 (1996); [https://doi.org/10.1016/0032-3861\(96\)81134-7](https://doi.org/10.1016/0032-3861(96)81134-7)
44. A.R. Polu and R. Kumar, *Int. J. Polym. Mater.*, **62**, 76 (2012); <https://doi.org/10.1080/00914037.2012.664211>